NASA SP-107

Symposium on PASSIVE GRAVITY-GRADIENT STABILIZATION

Ames Research Center
Moffett Field, California

May 10-11, 1965

NATIONAL AERONAUTICS AND SPACE ADMINISTRATION

17.

System Performance and Attitude Sensing of Three Gravity-Gradient-Stabilized Satellites

R. T. BEAL, P. H. CUDMORE,
R. H. KRONKE, AND P. G. WILHELM
U.S. Naval Research Laboratory

The advantages of a passive control system which alines a satellite axis along the local vertical prompted the U. S. Naval Research Laboratory (NRL) to flight-test three gravity-gradient control systems at low altitude (500 n. mi.). These systems were designed by the General Electric Co. Two 2-axis and one 3-axis stabilized satellites were flown to stabilize the controlled satellite axis to within ±10°. Attitude sensing was accomplished on all three satellites by nonoptimum earthlight detectors. In addition, the three-axis satellite had a magnetic and solar aspect system aboard. All satellites achieved low-eccentricity circular orbits of 500 n. mi. Raw, uncorrected data show that both of the 2-axis stabilized satellites have achieved steady-state alinement to the local vertical within 10°. Corrected data on a sufficient number of data points indicate alinement to the local vertical within 6°. Two intentional inversion maneuvers were successively completed with one of the 2-axis stabilized satellites. The mechanism for doing this was retraction of the gravity-gradient boom to half length, a coast phase, and reextension of the boom. No appreciable data were collected during these maneuvers, but alinement to the local vertical within 6° is known to have occurred within five revolutions after both maneuvers.

Many experiments to be flown in both military and civilian spacecraft may best be accomplished with one axis of the orbiting spacecraft alined vertically. In an effort to have vertical alinement capability in NRL spacecraft, the Satellite Techniques Branch has launched three gravity-gradient-stabilized satellites since January 1964. NRL flight-tested these systems to develop an operational control system with a pointing accuracy of ±10° which would be compatible with the standard NRL satellite structures. This action was taken independently of other gravity-gradient research programs to furnish the U.S. Navy a highly reliable, simple, low-cost, operational attitude-control system as soon as possible.

NRL GRAVITY-GRADIENT SATELLITE CONFIGURATIONS

The problem of satellite gravity-gradient stabilization breaks down into the major problem areas of: (1) Reducing all satellite tumble, (2) extending a boom or booms to achieve a large ratio of pitch- and roll-axis to yaw-axis moment of inertia, (3) damping the satellite librations to stabilize the satellite within tolerable oscillations, and (4) controlling the satellite boom-up or boom-down position. These experiments have successfully resolved all four problems. Not only can the pitch and roll axes be stabilized perpendicular to the local vertical, but the yaw axis can also be stabilized by proper selections of

pitch and roll moment-of-inertia ratios.

Experiment I (figure 1(a)) used a dumbbell configuration. The dumbbell was formed by an 80-pound satellite separated by a 28-foot boom from a 10-pound magnetically anchored viscous-fluid damper. Experiment II (fig. 1(b)) also used a dumbbell configuration consisting of a 130-pound satellite separated by a 41-foot boom from a 6-pound magnetically anchored eddy-current damper. The boom in this experiment may be retracted and reextended by ground command to invert the satellite. Because of the success of experiment I, the experiment II stabilization system was considered a flight test of an operational control system with the inversion capability carried as a new experiment. Experiment III (fig. 1(c)) used a different configuration from those of experiments I and II. It used three booms configured in a bent Y. The 130-pound satellite was at the center of the Y. The leg boom was bent out of the plane of the arm booms. All three

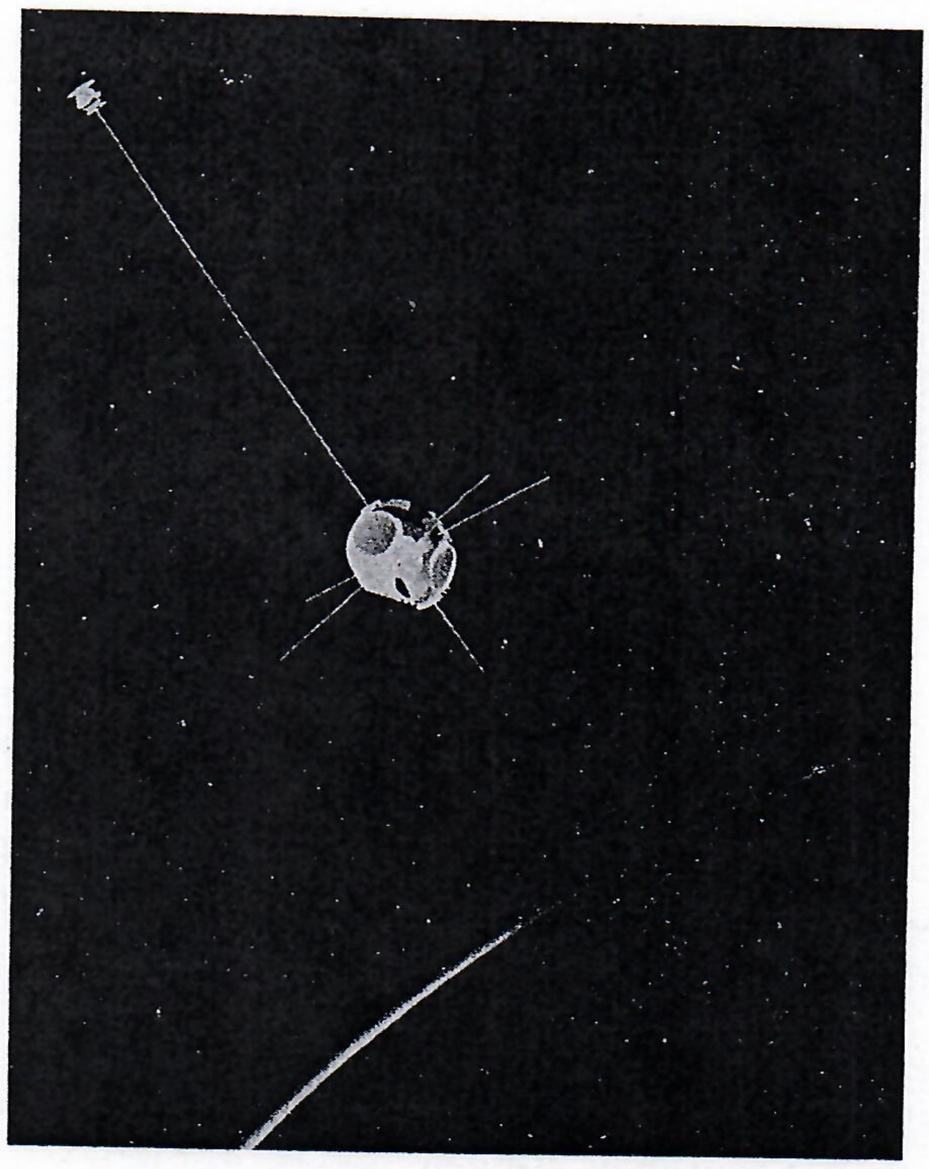

(a) Experiment I.

FIGURE 1.—Artist's conception of orbital configuration.

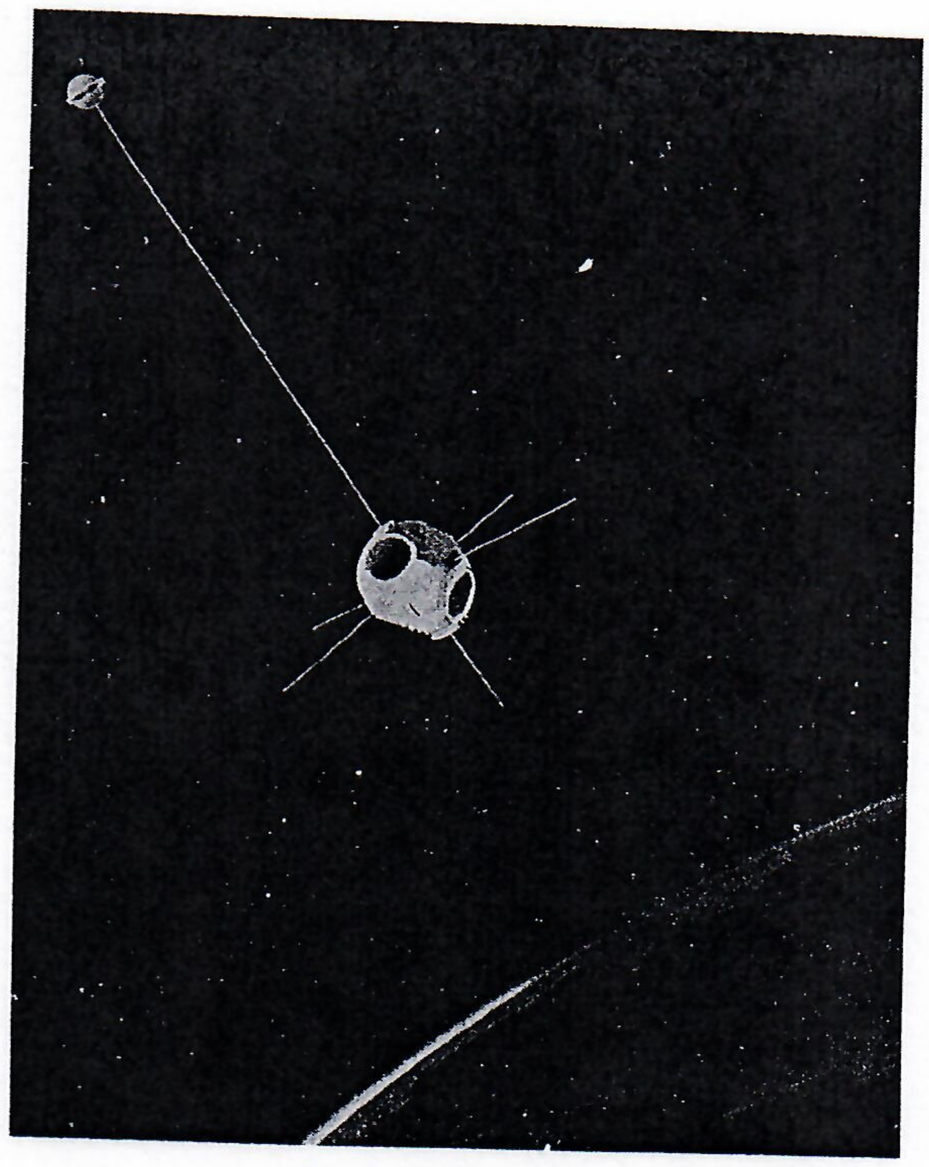

(b) Experiment II.

FIGURE 1.—Continued.

booms were 60 feet long. The arm booms each held a 2.9-pound tip mass. A 6-pound, magnetically anchored, viscous-fluid damper was attached to the end of the leg boom. This configuration is designed to give three-axis stabilization. Analytical studies and performance predictions on all three experiments were made by the General Electric Co. GE also designed and built the dampers. The booms were designed and fabricated by De Havilland Aircraft of Canada, Ltd.

All three systems were optimized for operating in 500 n. mi. circular orbits. Performance studies indicated that satellite pitch- and roll-axis alinement could be maintained better than the required 10° if eccentricity was low. Yaw-axis control was predicted to be 10° for experiment III. All three experiments achieved 70° inclination, 500 n. mi., circular orbits with eccentricities less than 0.002.

All three experiments used an Earth-albedo-detecting, optical aspect system. In addi-

tion to the optical aspect system, experiment III had magnetometers and a solar aspect system aboard. The pointing accuracy of experiments I and II may only be defined within the limits of the resolution associated with their respective aspect systems. Experiment III pointing accuracy may be defined totally as to the accuracy of the individual aspect systems by using combinations of the optical, magnetic, and solar instrumentation.

ATTITUDE INSTRUMENTATION SYSTEMS

Optical Attitude-Determination System

Design Limitations

First efforts toward selection of attitude-determining instrumentation systems were guided by the following limitations:

(1) There was only 90 days' lead time from conceptual design to flight hardware.

(2) Only a small amount of power was available—about 200 milliwatts.

(3) A high-reliability, long-life system was needed.

(4) Quick-look data reduction from telemetry was desirable.

The four possible candidate aspect systems were infrared, magnetic, solar, and earth-light detection. Infrared systems required too much power, typically involved moving parts which may be unreliable for long-term appli-

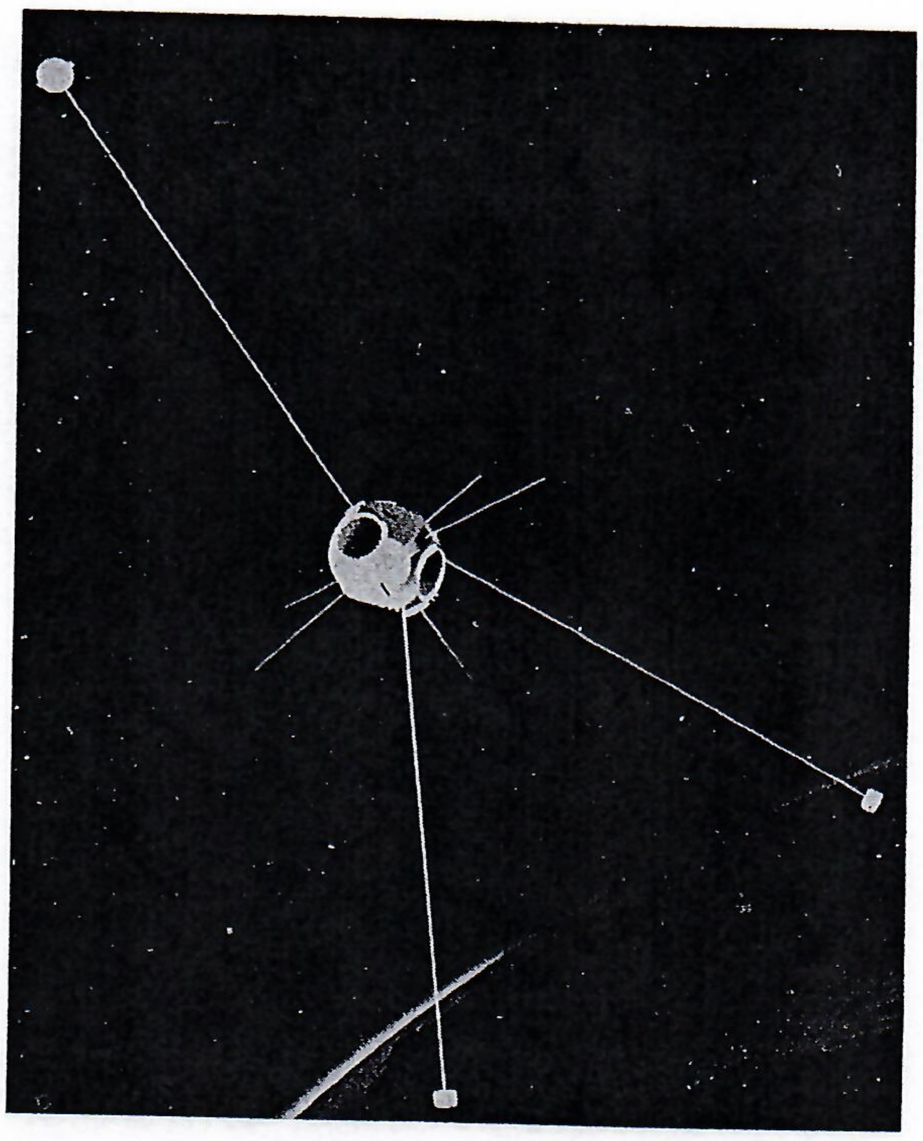

(c) Experiment III.

FIGURE 2.—Concluded.

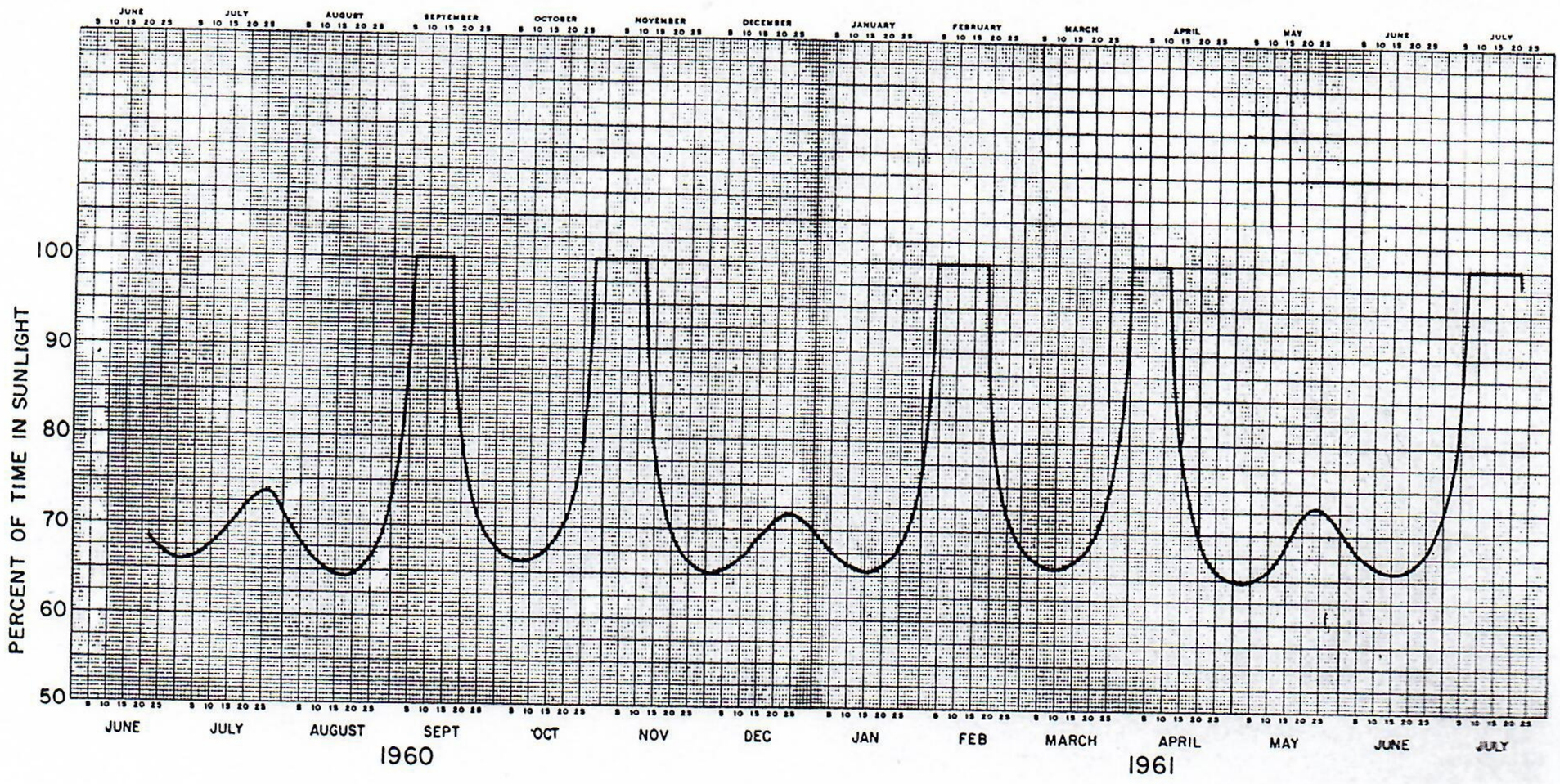

FIGURE 2.—Curve for 1960 Eta II satellite showing percent of time in sunlight for 1 year.

cations, and could not have been designed, constructed, and tested in the 90-day lead time. Both solar and magnetic systems required tedious computations. Therefore, the most practical method seemed to be a simple, optical, earthlight detection system.

General Optical-System Characteristics

For satellites launched to 500 n. mi. with a 70° inclination, the orbit plane precesses about the Earth in such a manner as to cause the satellite to be in direct sunlight from 66 to 100 percent of the time. Figure 2 shows this variation for experiment I. The satellite can "see" a fully illuminated Earth only during the valleys of this curve and can "see" a half-lit Earth continuously only during the peaks of the curve.

Figure 3 shows the geometry of the satellite-Sun-Earth relationships. Examination of the most favorable condition for optical coverage shows it to occur during the time when the orbital plane is parallel to the Sun's rays; this corresponds to the valleys of figure 2. At this time the Earth is fully illuminated, as seen by the satellite, 33 percent of the time (one-third of an orbit).

Examination of the least favorable time for optical coverage shows that it occurs when the orbital plane is perpendicular to the Sun's rays; this corresponds to the peaks of figure 2. At this time the Earth is always only half illuminated, as seen by the satellite. However, by using three banks of optical detectors (sectors), spaced 120° from one another, fair conditions still exist for optical coverage at reduced resolution provided that two of the three sectors view the illuminated half of the Earth. For a satellite without yaw stability, this condition should exist 67 percent of the time (two-thirds of an orbit).

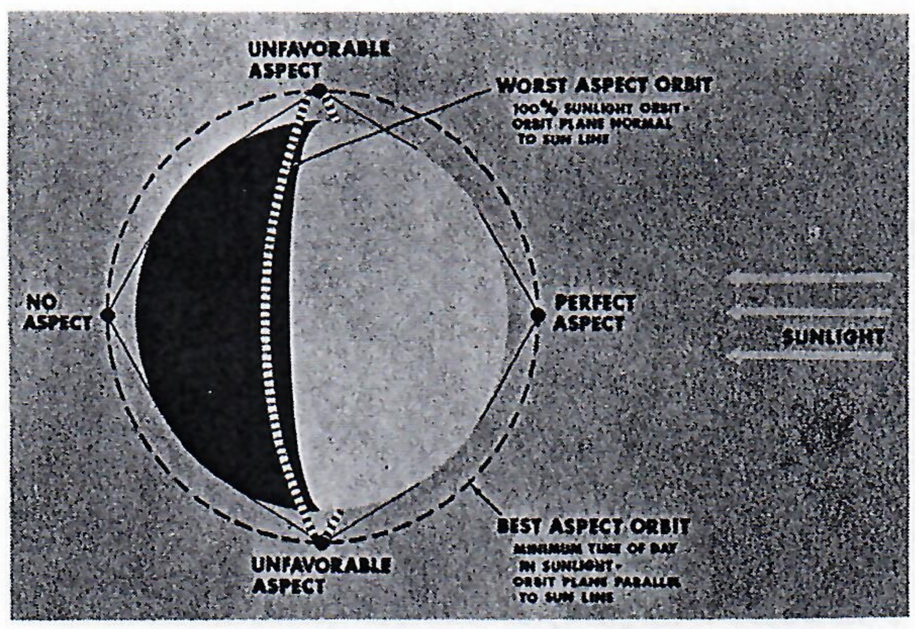

FIGURE 3.—Satellite in good and bad lighting.

Experiment I

First Generation Flight Hardware

Figure 4 shows diagrammatically the optical-detector look angles and relative hardware positioning in the satellite for experiment I. Because it was not known whether the satellite would stabilize with the boom up or with the boom down, three sectors were mounted on the top hemisphere and three, on

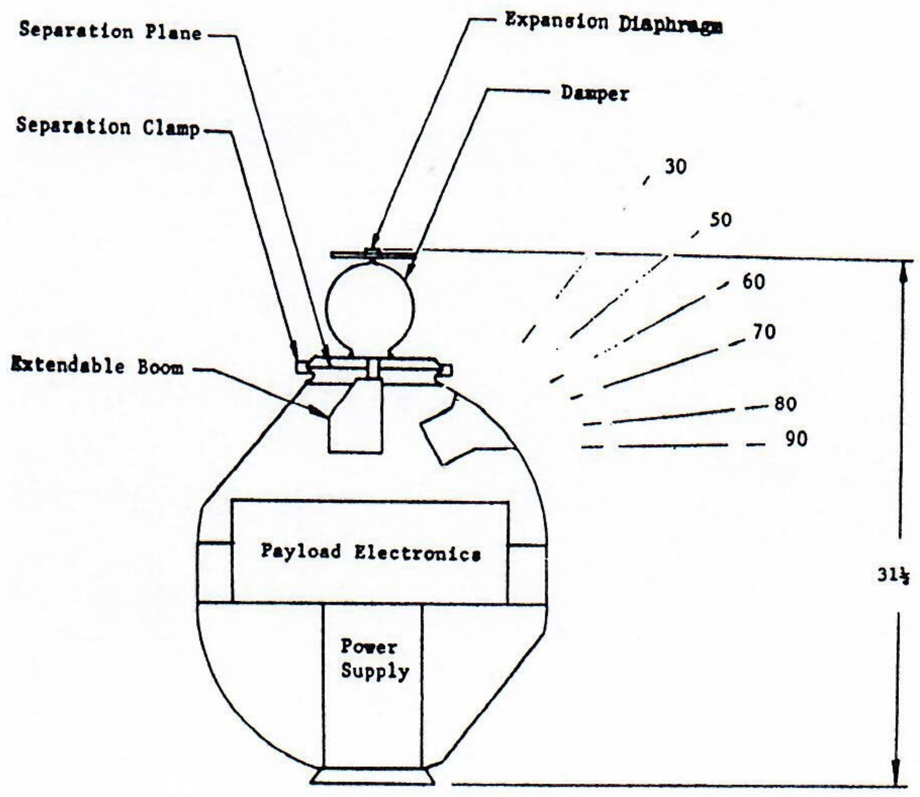

FIGURE 4.—Geometry for experiment I.

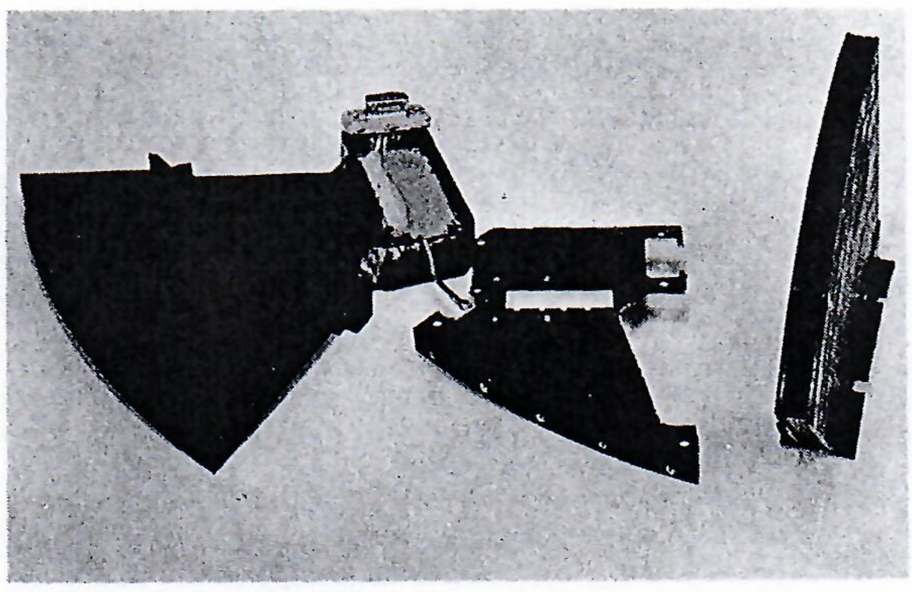

FIGURE 5.—Optical aspect sensor for experiment I.

the bottom hemisphere. These sectors are spaced 120° from one another in a plane parallel to the satellite equator. Each sector has five individual detectors separated by collimating walls. Figure 5 is a photograph of a flight backup sector. The sector is mounted flush with the satellite skin, and the nylon extenders, which were added to achieve better collimation, were mounted external to the skin. The light bulb included in each sector would illuminate the detectors upon radio command and thus provide open- or short-circuit failure mode information.

The optical detectors used were Texas Instrument Co.'s LS400 silicon planar photo transistors whose spectral response peaks at 0.9 micron. Figure 6 shows the relative spectral response of this transistor.

Figure 7 is a block diagram of the system. Power energizing all of its individual detectors is switched to one sector at a time. This makes it possible to time-share one common set of Schmidt Trigger circuits and minimize power drain (the entire electronics system required 80 milliwatts of unregulated power). The outputs from the Schmidt Triggers are combined with a simple resistor network whose output voltage at any time is characteristic of the number of detectors in a particular sector that are illuminated by earthlight. This output voltage is then impressed on a subcarrier oscillator in the telemetry system. The sampling rate of the system is such that it samples all six sectors in 4 seconds on a continuous basis. The sample rate is controlled by a simple two-transistor astable multivibrator. Figure 8 is a detailed schematic diagram of the system electronics. Basically, earthlight illuminates an LS400 transistor and it produces current flow into its transistor amplifier which further amplifies this current and routes it into the 100-kilohm sensitivity-controlling resistor which develops a voltage at the input to a Schmidt Trigger. When this voltage exceeds the threshold, the first transistor of the Schmidt Trigger turns on and the second transistor turns off with regenerative action. This produces a voltage-level change at the Schmidt Trigger output from ground to 6 volts which is applied to the resistive network; the net result is to add 1 volt to the output signal for each illuminated detector in a sector. Thus, the output voltage can be any one of six discrete levels of 0, 1, 2, 3, 4, or 5 volts, depending on the incident illumination on the sector. Two additional areas deserve mention here. First, since the detectors are exposed to radiation, the switching of power off and on gives them a chance to anneal and minimize radiation-induced changes; and, second, the LS400 transistors and their individual amplifying transistors were selected such that their combined leakage currents at 60° C provided a margin of

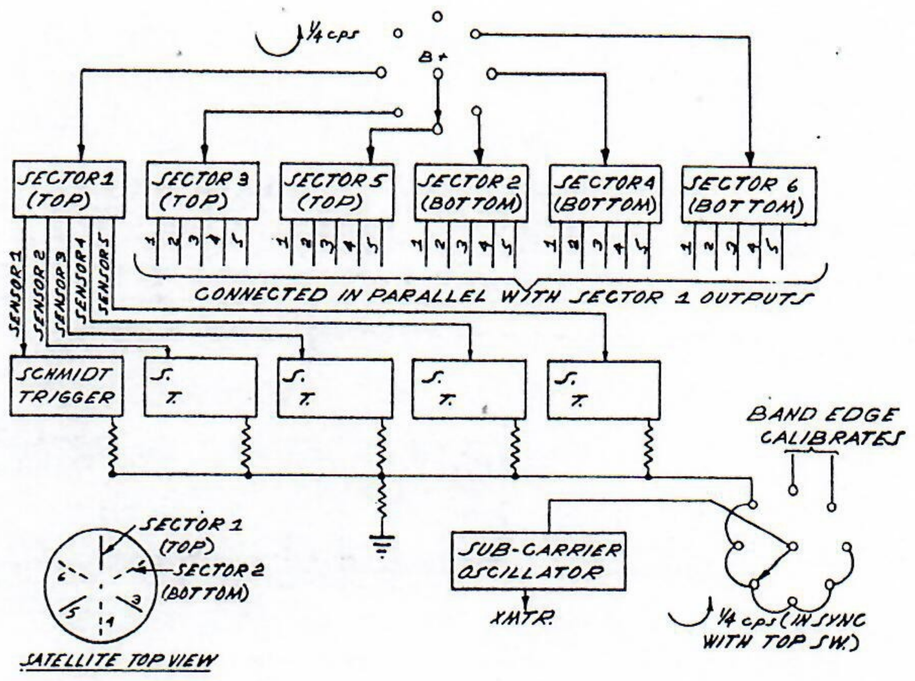

FIGURE 7.—System block diagram for experiment I.

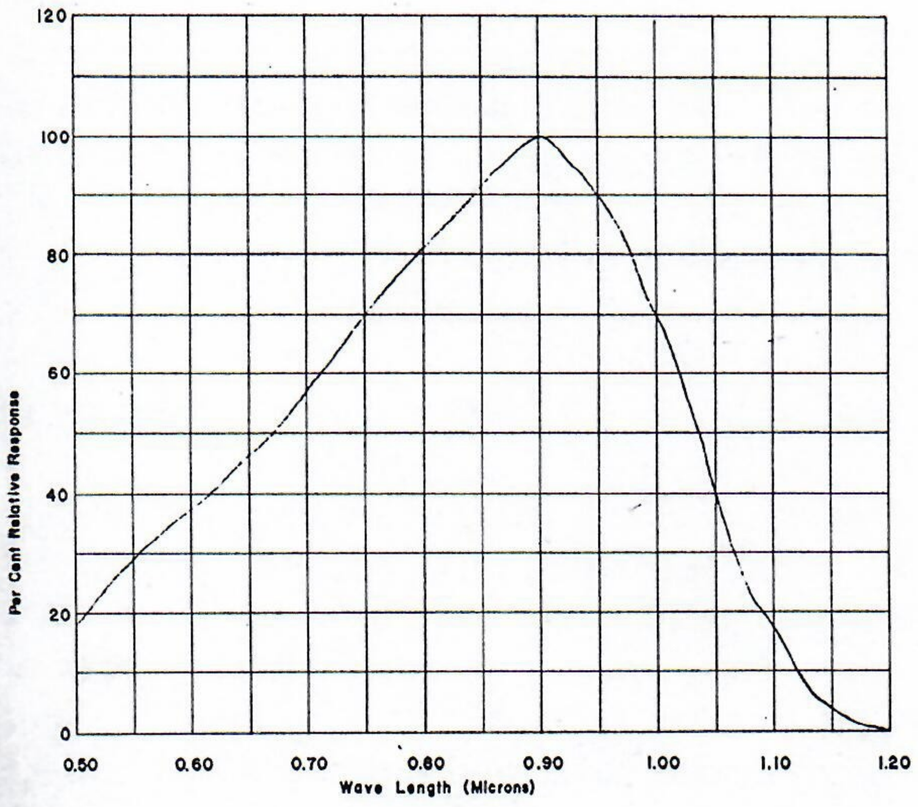

FIGURE 6.—Spectral response curve for LS400 curve.

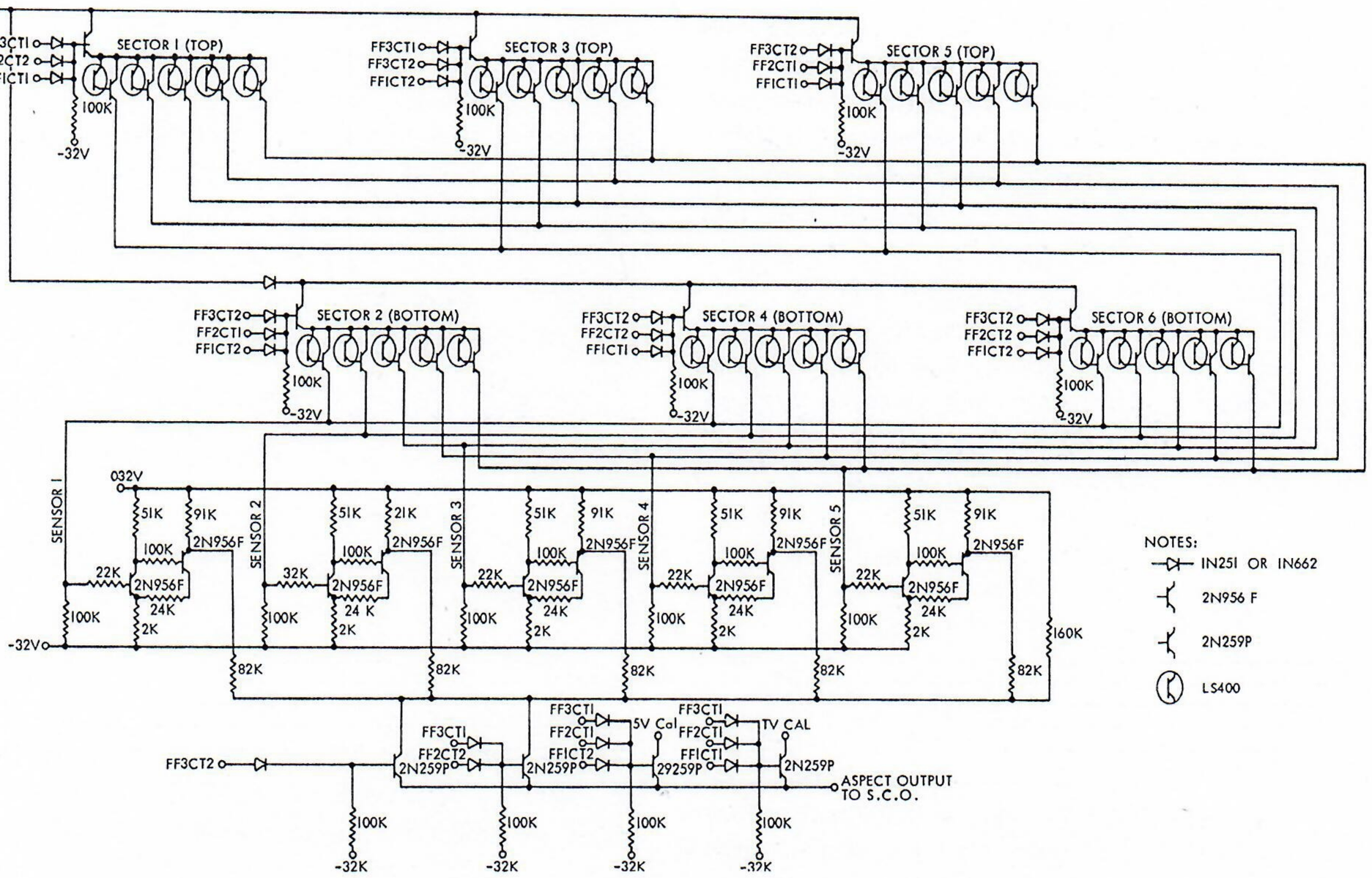

FIGURE 8.—Electronics schematic for Earth aspect system of experiment I.

at least 10 to 1, and typically 25 to 1, between light-induced currents and thermal-induced currents. Apparently this design philosophy is sound since this system has been working in orbit for 18 months without any indication of malfunction.

Quick-Look Data Reduction

This system is capable of quick-look data reduction. Figure 9 shows the geometrical relationships. When the Sun is directly above the satellite, it is possible to regard the Earth as an illuminated two-dimensional disk as viewed from beneath the satellite. By looking in the other direction, it is possible to regard the spherical satellite as another two-dimensional disk with light sensitive areas. Both of these plane surfaces effectively represent look angles—to the horizon in one case and optical beamwidths of the light detectors in the other case. Figure 10 shows these plane surfaces. The satellite plane is typical of experiment I, but not exact. By superimposing these templates and moving one relative to the other it is possible to simulate accurately the satellite's motion about the local vertical for tilt angles up to 30° at 500 n. mi. This two-dimensional model becomes inaccurate for large tilt angles. It is necessary to measure only the distance between the centers of

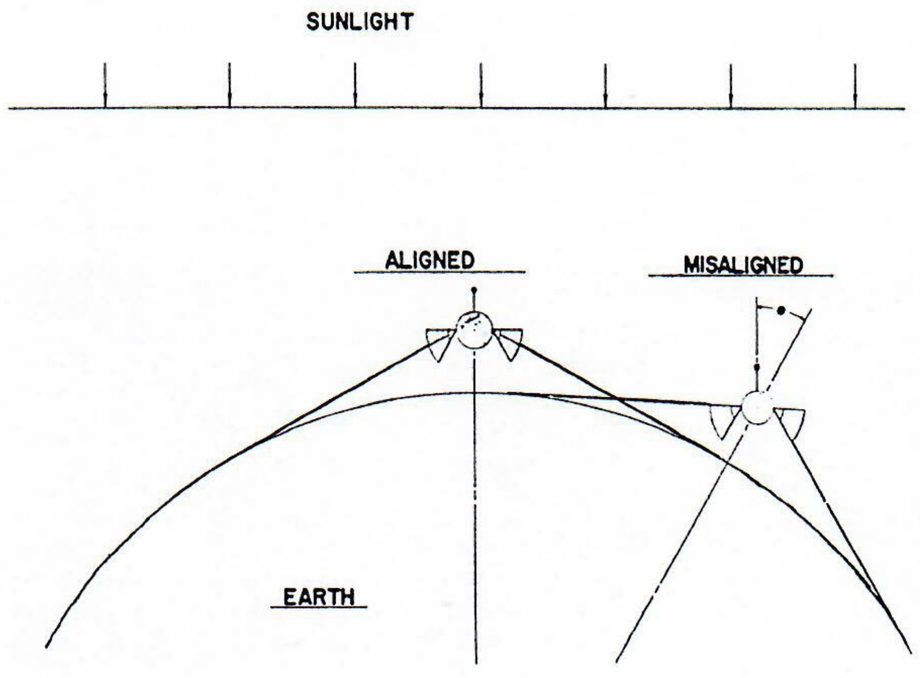

FIGURE 9.—Satellite-Earth "look" angles.

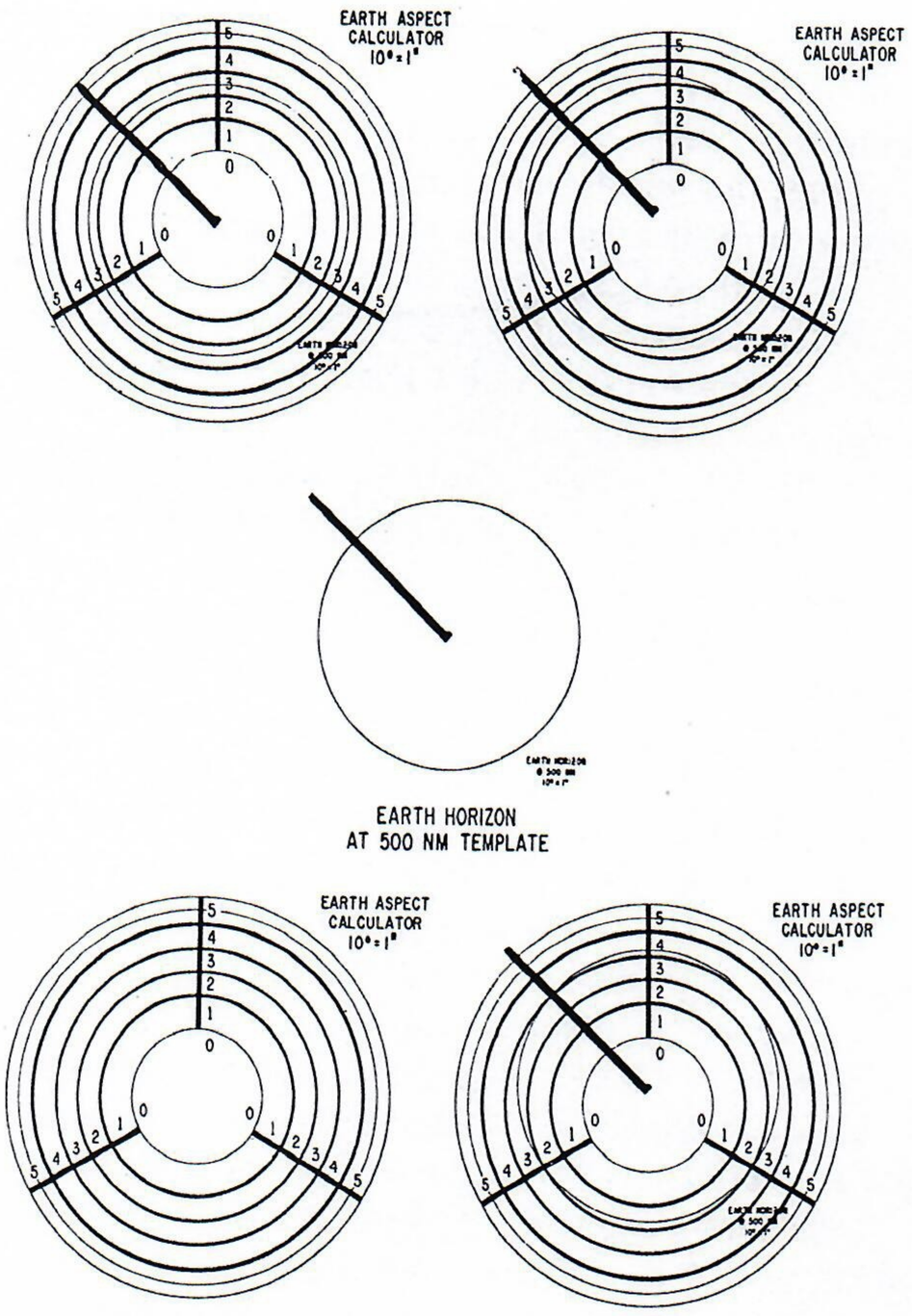

FIGURE 10.—"Quick-look" data-reduction templates for experiment I.

the disks to determine the tilt angle when the Earth disk is placed relative to the satellite disk to produce the observed telemetry reading. Figure 10 also shows the templates in a few typical positions. The 333-reading shown in the upper left-hand corner of figure 10 corresponds to earthlight illuminating three of the detectors in each of three sectors. This telemetry indication shows that the satellite is alined to the local vertical at a tilt angle somewhere between 0° and 6° about a cone of ambiguity.

The 334-reading indicates tilt alinement between 3° and 8°; the 234-reading, 6° to 16°. A summary of possible readings at 500 n. mi. is given in contour-chart form in figure 11. Thus, this system is capable of only limited resolution but does provide the essential information simply and reliably. During 100-percent-sunlight phases, the data are still usable if two sectors "see" the illuminated portion of the Earth, but the resolution decreases still further. For example, the 333 and 334 telemetry indications could degenerate to 300 and indicate alinement to the local vertical between 0° and 8°. In similar manner, the 334 and 234 telemetry indications could degenerate to 340 and indicate alinement between 3° and 17°.

Deficiencies of Experiment I

The deficiencies of experiment I are as follows:

(1) We cannot from telemetry information determine which detectors in a sector are illuminated but only the total number.

(2) Because of payload volume constraints, the collimating tubes could not be made long enough to provide optical beamwidths independent of albedo variations.

EXPERIMENTS II AND III

Second Generation Flight Hardware

With the results of the optical system of experiment I providing valuable hindsight, the design of the more refined optical system for experiments II and III was undertaken.

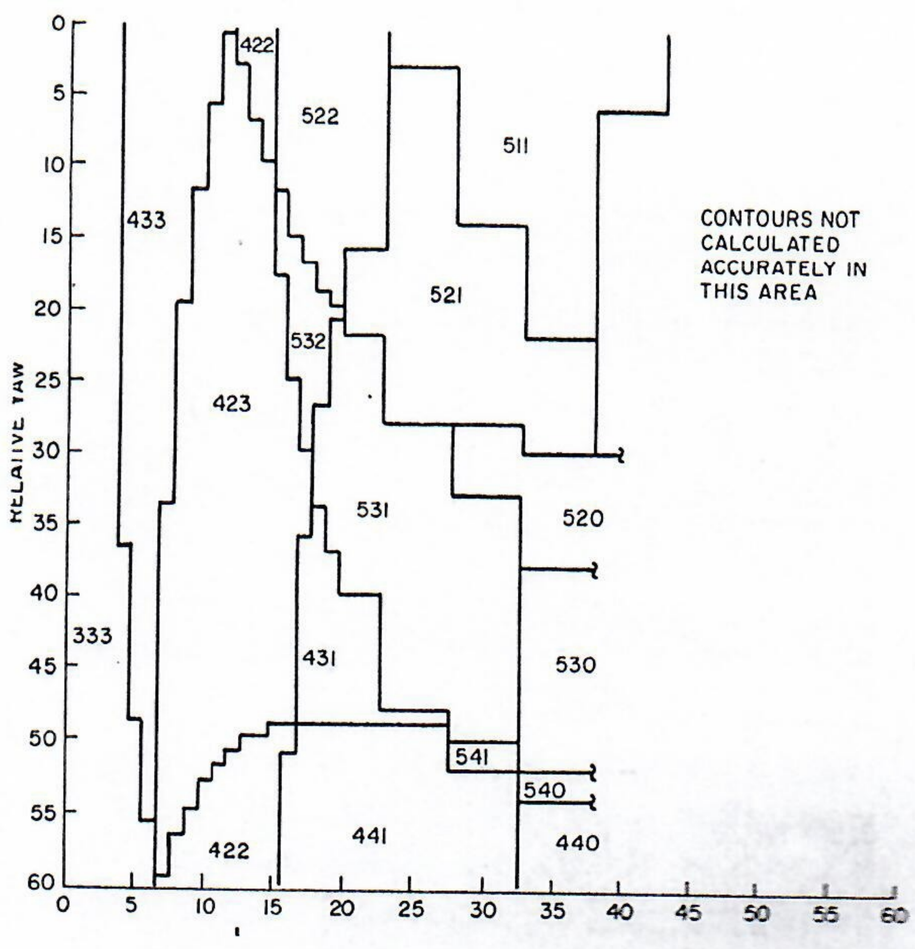

FIGURE 11.—Contour chart for experiment I.

The following criteria were established as guidelines:

(1) Maintain basically the same reliable low-power-drain design which is capable of quick-look data reduction

(2) Provide digital weighting of detector responses to determine the condition of each individual detector

(3) Provide better optical collimation while maintaining triggering ability on the Earth's dimmest spots and a maximum of 1° cone beamwidth angle on the Earth's brightest spots; this characteristic would enable resolution at the contour edges to within ½°

(4) Assume near-perfect launch-vehicle operation and optimize the system for altitudes ranging from 400 to 600 n. mi.

(5) Provide essentially a system whose resolution follows the equation:

$$\text{Resolution} = 1/3 \text{ tilt angle}$$

With the aid of Mr. A. J. Martin of NRL and the NARAC digital computer, eight separate proposed sensor geometries were evaluated. The sensor geometry shown in figure 12 proved most desirable. As can be seen the major changes are in the look angles of the detectors and in the increase in the number of detectors in a sector from 5 to 12. Three sectors were again placed on each hemisphere, as in experiment I. Figure 13 is a photograph of a flight backup sector.

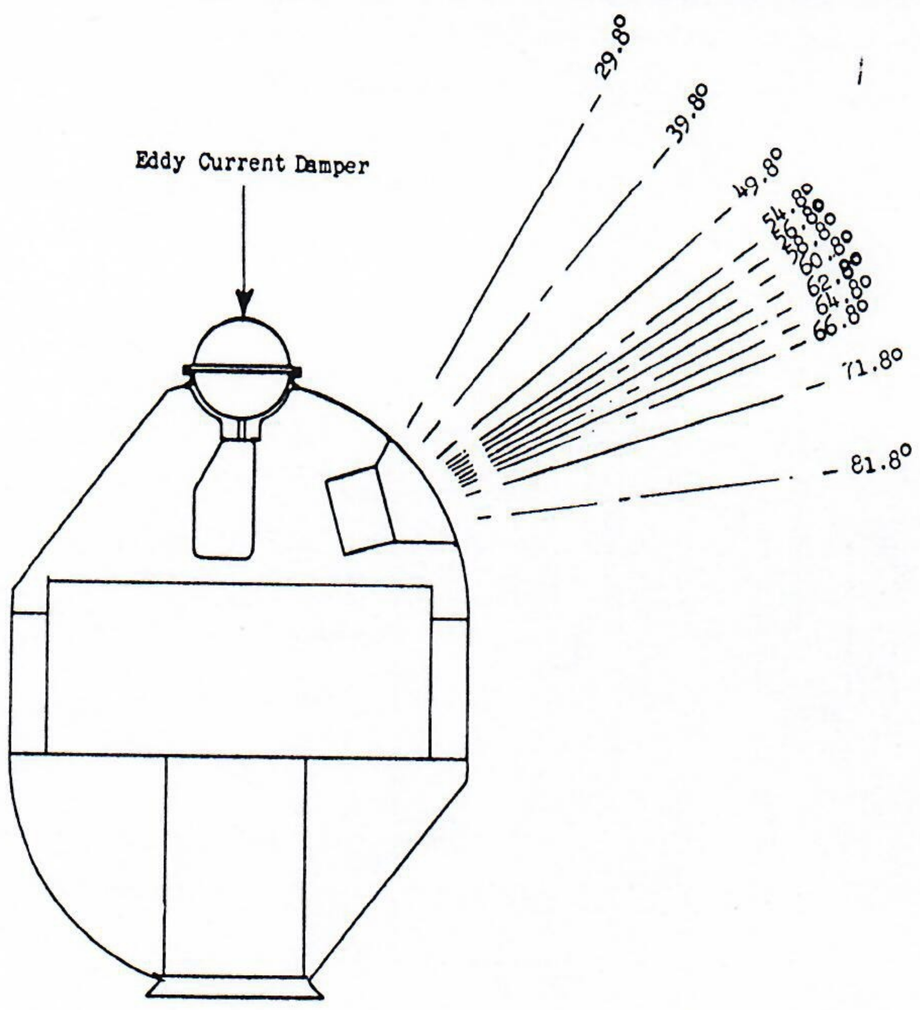

FIGURE 12.—Geometry for experiments I and II.

Figure 14 is the block diagram of the system electronics. As can be seen, it is similar to the experiment I system except in the following respects:

(1) The system sampling rate is 8 seconds per frame instead of 4 seconds per frame.

(2) Provisions are made for digital weighting of the output to the telemetry system. This necessitates supercommutation of the 12 detectors in groups of 3 each during the time power is applied to any particular sector; the resulting output telemetry voltages have nine discrete levels of 0, 0.5, 1, 1.5, 2, 2.5, 3, 3.5, and 4 volts depending on sector illumination conditions.

Figure 15 shows the detailed electronic schematic. The major differences between this schematic and the one for experiment I are that this one has more parts and that it draws more power (1/3 watt). However, the higher power drain was a result of insufficient development time and is not an inherent higher power demand. The power drain can be reduced to 80 milliwatts by the addition of 4 transistors and 12 diodes to supercommutate the power applied to the 12 Schmidt Trigger circuits in groups of 3 synchronously with the supercommutation of the detectors in an individual sector.

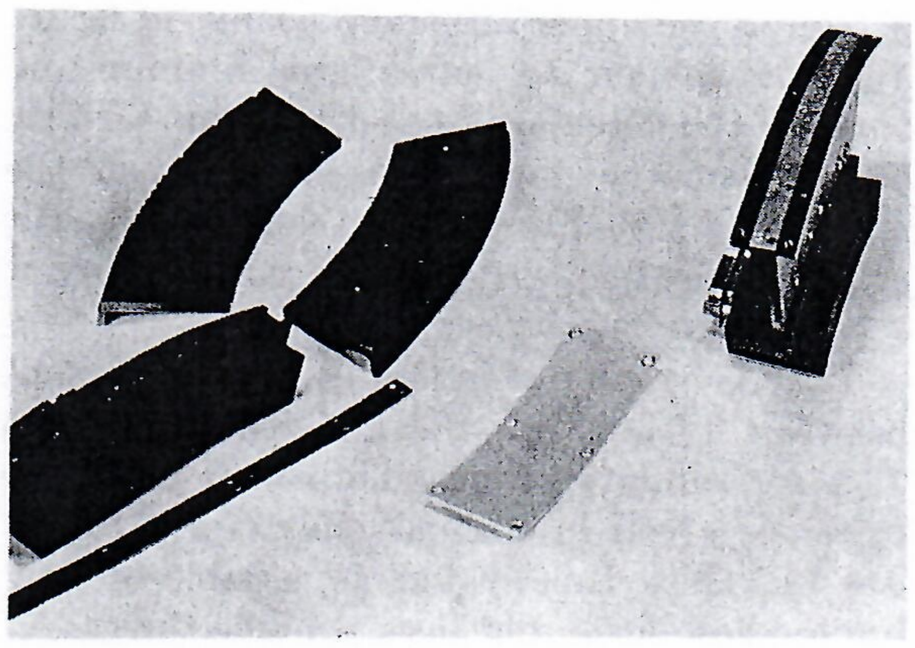

FIGURE 13.—Optical aspect sensor for experiments II and III.

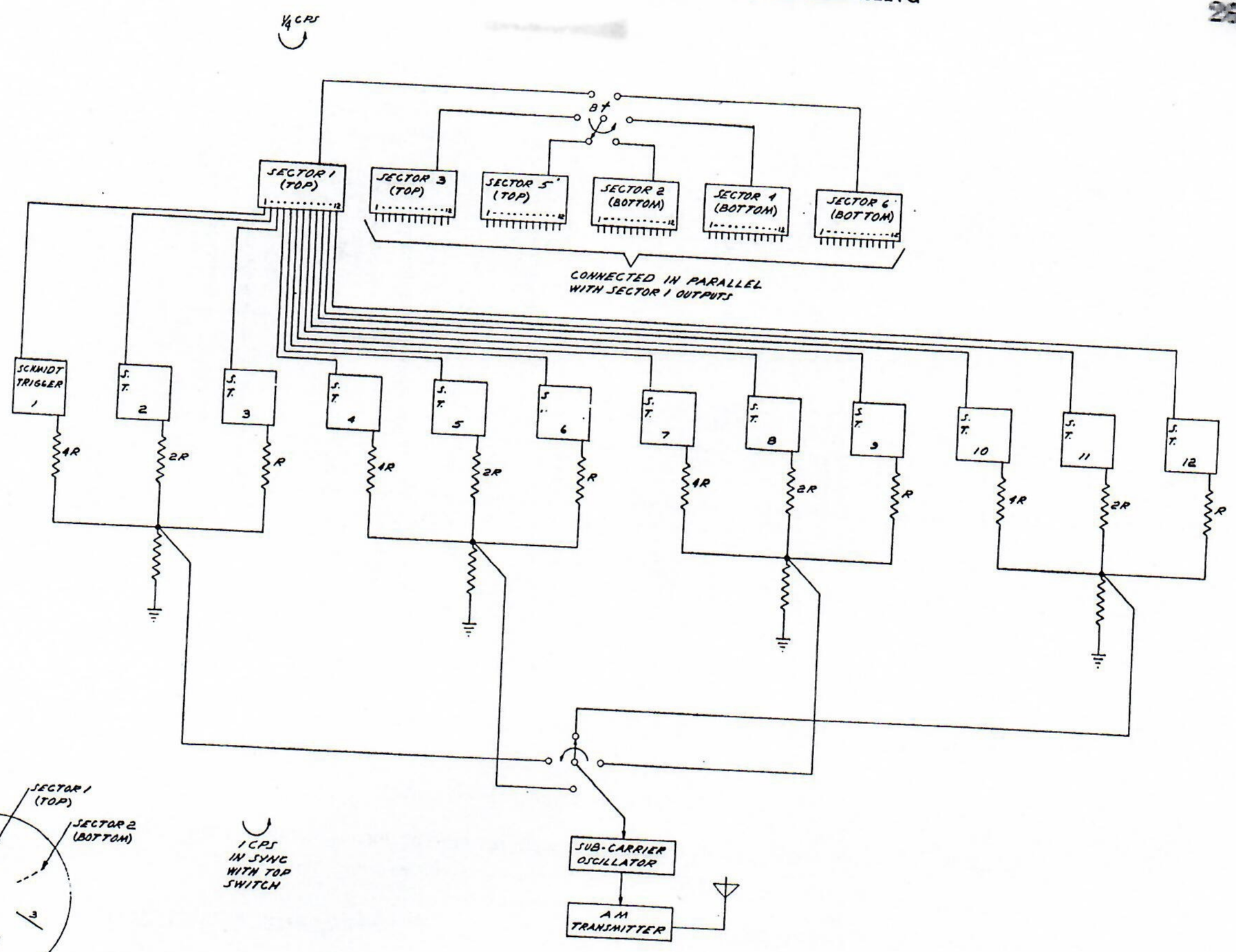

FIGURE 14.—Optical system block diagram for overall system electronics of experiments II and III.

Figure 16 shows the increased resolution attainable with this system. It can be seen that there are about five times more possible outputs and resolution is greatly increased over that of experiment I.

In addition, there was provided, only on experiment II, a linear albedo-measuring detector with characteristics the same as those of the optical-system detectors. This detector views the area vertically below the satellite and is capable of measuring albedo variations from 0.1 to 0.8 in the 0.9-micron region.

System Deficiencies

It became apparent after the launch that the sensitivity setting of the detectors was marginal. This was evidenced by the fact that some detectors viewing the illuminated Earth continually turned on and off during the 15-minute observation period of one ground station. The rate at which this occurred was much too fast for the natural oscillation frequencies of the gravity-gradient system.

The condition of marginal sensitivity is further borne out by the telemetry observations from the linear albedo detector included in experiment II. The data very rarely indicate an albedo higher than 0.10. All optical-system detectors were set to trigger at albedos between 0.02 and 0.07. There have been rare occurrences when the albedo reached a peak of about 0.15 as measured by the linear detector. Fortunately, time analysis of the telemetry data enabled us to reduce the data at reduced resolution.

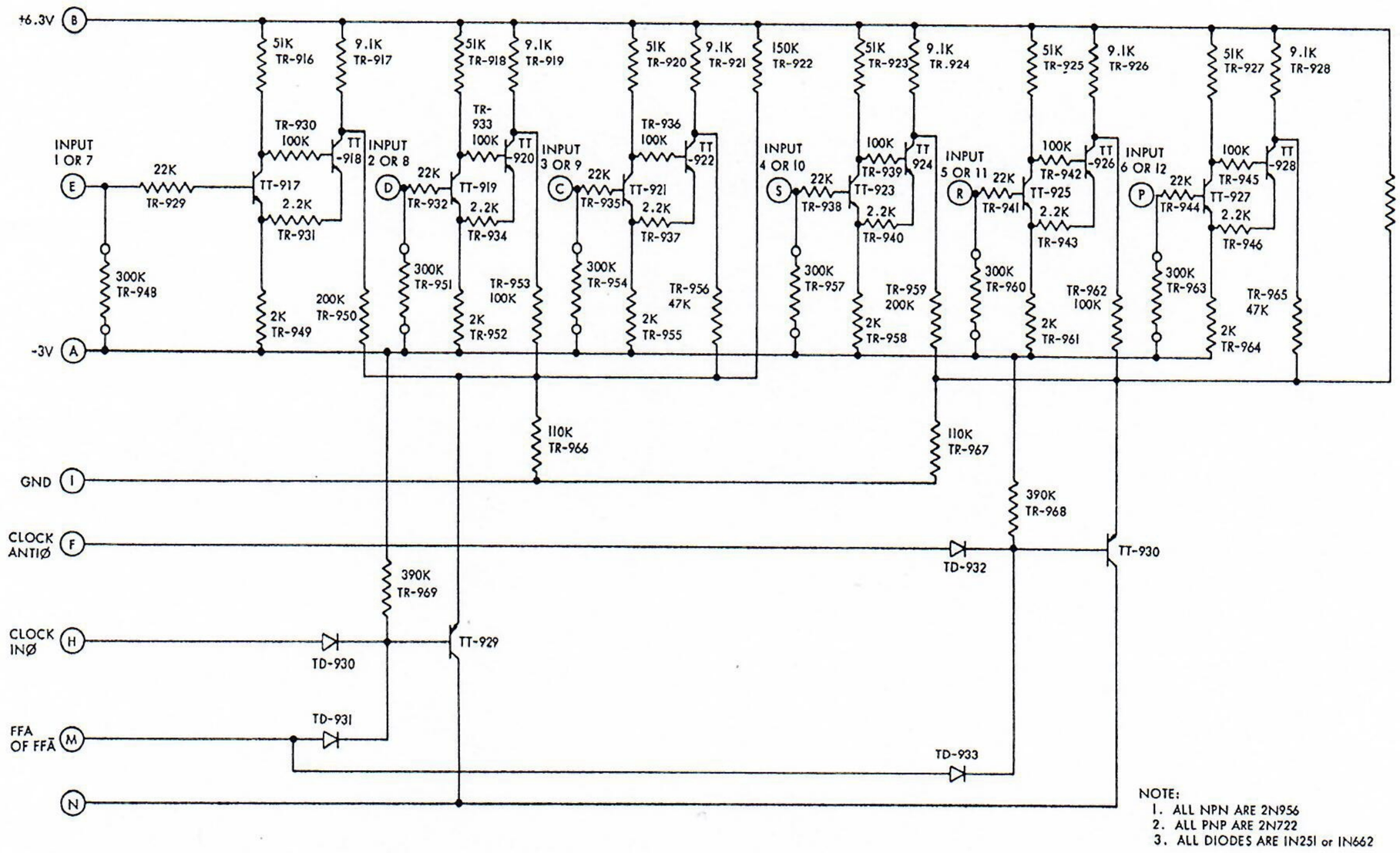

(a) Part I of connecting circuitry.

FIGURE 15.—Optical system electronics schematic for experiments II and III.

FUTURE OPTICAL EXPERIMENT

Four visible-light detectors with analog outputs have been installed in a spin-stabilized satellite which is in the final stages of launch preparation. Each of these detectors has different characteristics and spans a great enough sensitivity range to determine whether a fixed-sensitivity, visible-light detector is entirely satisfactory for attitude determination purposes.

ADVANTAGES OF OPTICAL SYSTEM

The advantages of an optical attitude-determination system are as follows:

(1) It is simple and highly reliable

(2) It provides quick-look data reduction

(3) It requires very little power (less than 1/10 watt)

(4) It is capable of good resolution

(5) It is inexpensive; cost for the instrumentation systems in experiments I, II, and III was about $10,000 each.

Magnetic Aspect System

The magnetic aspect system flown on experiment III is a "Three-Axis Fluxgate Magnetometer" built by the Schonstedt Instrument Co. It is an excellent instrument which is highly reliable, stable, and accurate, draws low power, and has performed flawlessly both in tests and in flight.

The equation describing the output voltage of each axis is $E = 5\ H \cos \theta$, where E is the output in volts, H is the magnitude of the magnetic field in gausses, and θ is the angle between the magnetic-field line and the axis of the magnetometer. At an orbital altitude of 500 n. mi. a full-scale sensitivity of 0.50 gauss was chosen. This has proven to be a fortunate choice since readings as high as 0.44 gauss have been noted.

Calibration coils on each magnetometer axis are an important feature of this instrument. On command, a known field of plus, then minus, 0.20 gauss is applied to check that no change in sensitivity has taken place. Since the three axes are orthogonal, another

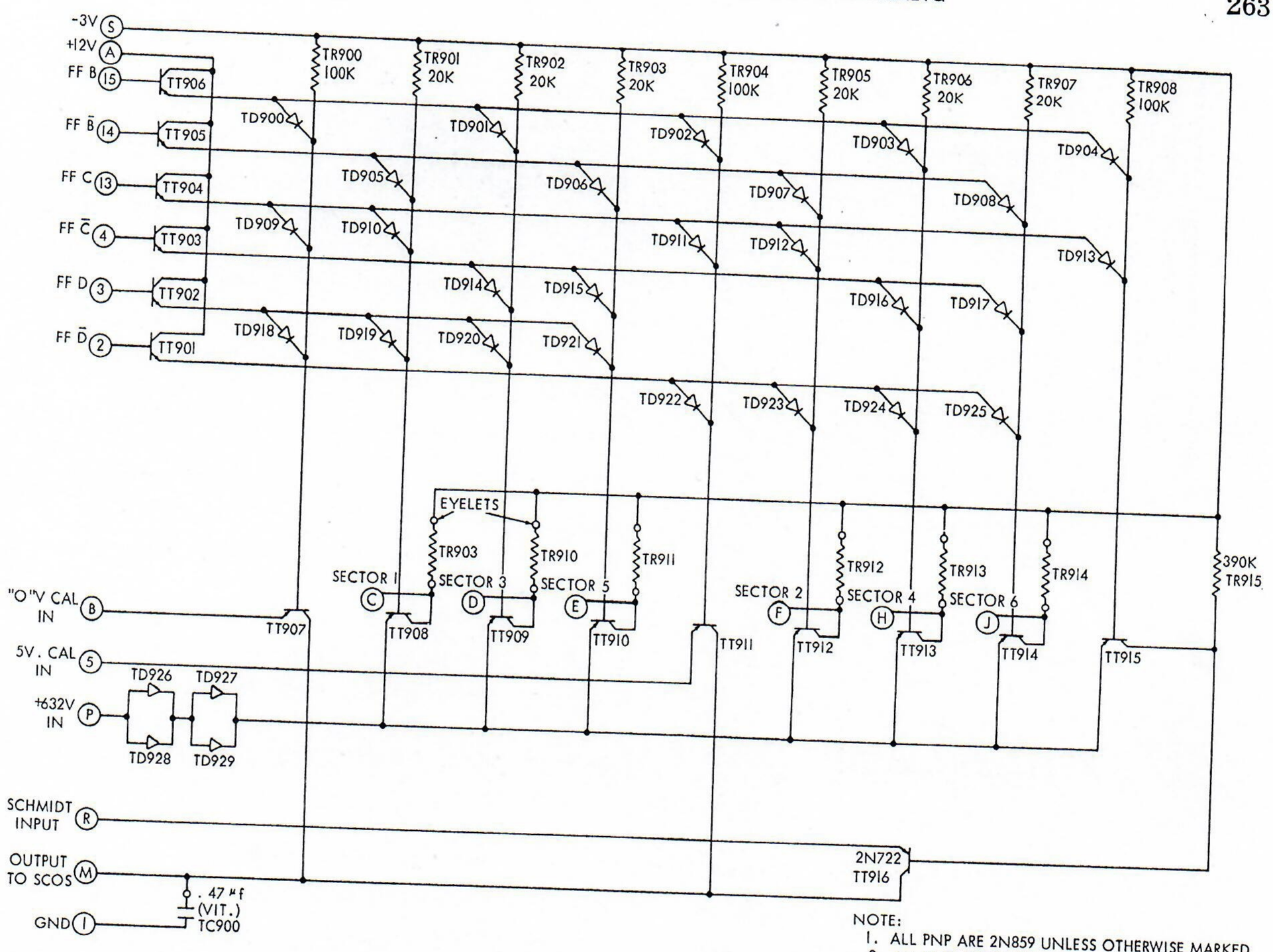

(b) Part II of connecting circuitry.

FIGURE 15.—Concluded.

method of checking the accuracy of the readings is to take the square root of the sum of the squares and compare it with the computed value. This computed value comes from the U. S. Naval Weapons Laboratory's "Stretch Computer" and is a mathematically derived "magnetic model" of the Earth. The limitations of magnetic aspect are accurate knowledge of the Earth's magnetic field in space which is believed to be known better than 5 percent and resolution of the telemetry system. Another limitation of magnetic aspect data is that it cannot be reduced without a fairly involved computer program. This virtually rules out any "quick-look" or hand-reduced data. An advantage of the magnetic aspect system is that data are available 100 percent of the time. With magnetic aspect alone a maximum and a minimum tilt angle can be determined.

Solar Aspect System

The solar-aspect system is extremely simple. Six strings of 11 solar cells each are placed on the satellite in an orthogonal system. The planes of the six solar-cell strings form a cube. The voltage output from the solar cells, when properly loaded, very closely follows a cosine curve as the incident angle varies from normal to grazing angles. Therefore, the solar aspect system produces data similar to that of the magnetic aspect system. Both systems measure the direction cosines between their own orthogonal coordinate system and the solar or magnetic vector. The solar aspect system of course has limi-

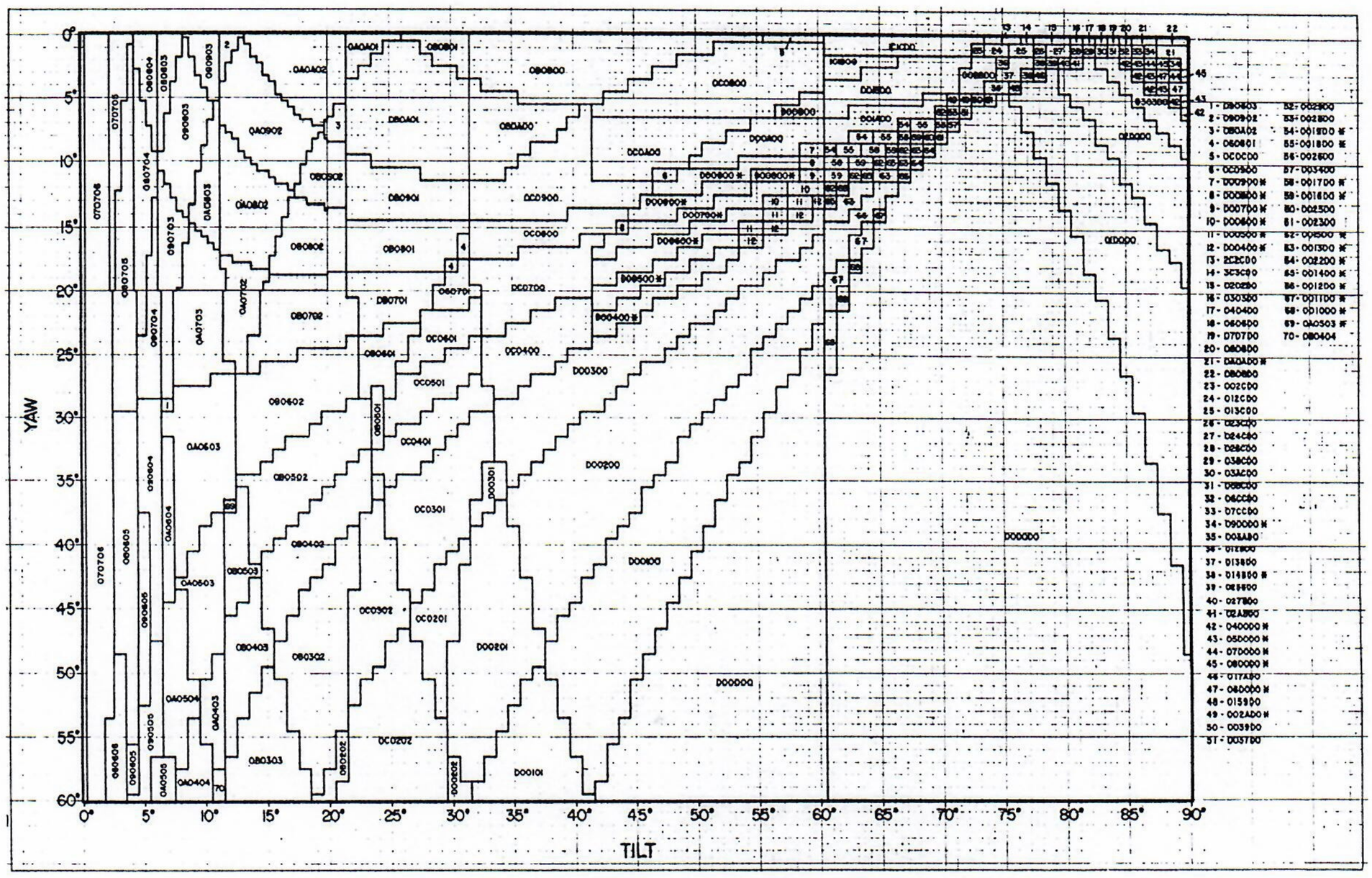

FIGURE 16.—Contour chart for experiments II and III.

tations also. Earthshine is the most serious. However, since the Sun's magnitude is so accurately known and is constant, only accurate readings from two solar cells are required to determine the direction cosines. The two largest value readings are used for this calculation. For a solar cell looking straight at a sunlit Earth the output voltage can only be approximately 10 percent of a full Sun reading. For most orientations of Sun, satellite, and Earth, earthshine is not nearly so great a problem as one would think initially. At times, large readings due to reflections have been observed. At other times, small readings due to shading have been observed. The reflections and shading are due to the fact that booms and antennas protrude from the payload. Fortunately, these conditions occur only a small percentage of the time and usually do not last for more than a minute. Another limitation which we have not yet been able to evaluate, because of the short time in orbit, is the effect of radiation. If radiation affects all solar cells equally, it will not affect the overall system performance. If the cells are affected unevenly, they will have to be recalibrated. This can be done on one cell at a time when that cell is normal to the sunline. Still another limitation is that the output voltage is a function of temperature as well as of aspect angle. Therefore, temperature sensors had to be included for each solar cell in the system.

To summarize, the solar aspect system performs remarkably well within the limits of our analog telemetry system. Equally important is that, by using the square root of the sum of the squares as a confidence factor, it is quite simple to exclude bad data points due to earthshine, reflections, or shading.

Combination Systems

The primary purpose of flying more than one aspect system on experiment III was to get total aspect. It is impossible to get total

aspect from any one of these aspect systems. A second system is always required to resolve the ambiguities. Generally speaking, angles such as direction cosines must be measured between the spacecraft and two nonparallel vectors, such as the magnetic-field line and the sunline or the magnetic-field line and the local vertical. Since three independent aspect systems were flown, three possible combinations are available for total aspect: optical and magnetic, optical and solar, and solar and magnetic. Most of our data are taken from the solar-magnetic combination. Figure 17 shows the relationship between the solar, magnetic, and satellite coordinate systems. Axes 1 to 6 are solar; axes X, Y, and Z are magnetic; and yaw, pitch, and roll are the satellite axis. Other combinations will be spot-checked as a matter of interest and as a cross-check on the data. Conceptually, the problem of taking the raw data and translating into useful aspect information is simple and straightforward. Practically, it is a long, involved process requiring extensive computer calculations. NRL has been fortunate to have the able assistance of the Analysis and Computation Division of the U. S. Naval Weapons Laboratory (NWL) at Dahlgren, Va.; the entire program was written there and all of our three-axis data were reduced there.

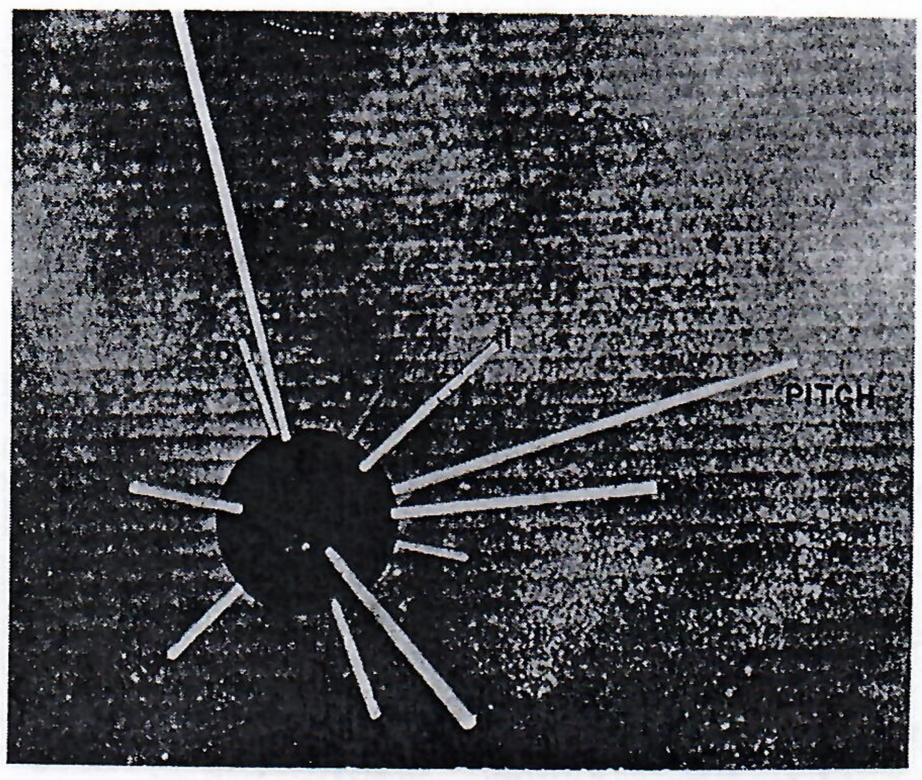

FIGURE 17.—Satellite coordinate systems for experiment III.

PERFORMANCE DATA

Experiment I

Satellite-separation tip-off rate was damped during the 12 orbits between satellite–launch-vehicle separation and boom extension. At the time of boom extension, the boom axis was $20° \pm 5°$ off the vertical; the inertial rate was essentially zero. These initial conditions represent an initial oscillation of about 40° half-amplitude after boom extension. Because of the nature of the optical instrumentation system, it is not possible to determine if the 20° offset was all pitch or a combination of roll and pitch. Each of the extremes, a 20° pitch error and a 20° roll error, was run in the GE digital simulation program under the assumption of nominal damper performance to provide final predictions of the oscillation decay. The data obtained during the 3 days following boom extension were completely consistent with the predictions (see fig. 18) and steady-state motion with peak errors of less than 6° was reached in less than 3 days.

During the first 3½-week period after launch, earthlight conditions were optimum for optical information. Data from this period have been analyzed in great detail. Each data point has been reviewed to insure the correct satellite subpoint lighting condition. These data cover orbits 26 through 261 and amount

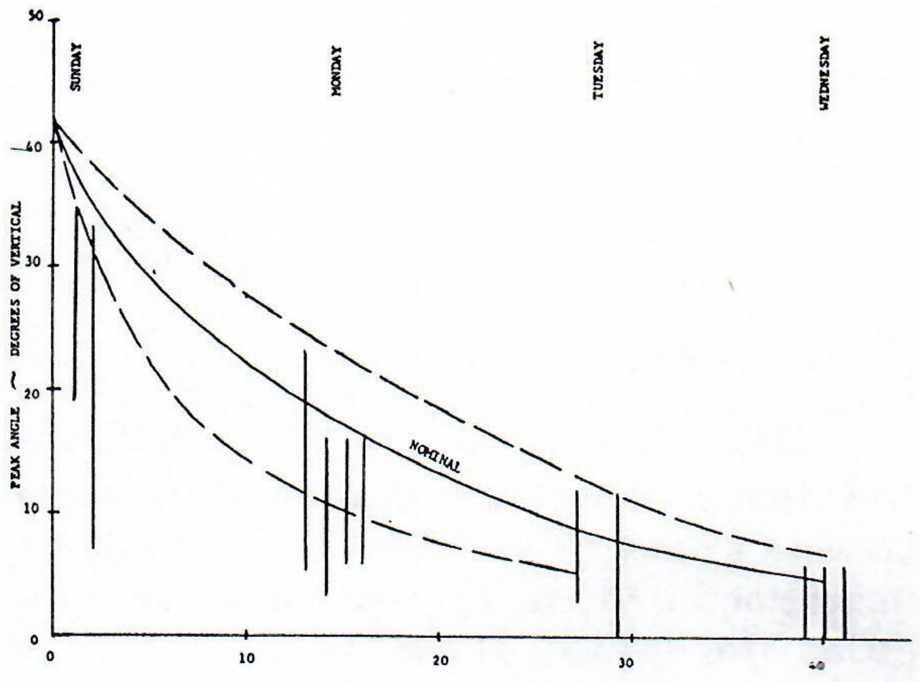

FIGURE 18.—Decay performance for experiment I.

to 6 hours 37 minutes and 51 seconds. So that samples could be obtained from as many varied stations as possible, data were collected by Hybla Valley, Va.; South Point, Hawaii; Lima, Peru; San Nicholas Island, Calif.; and Woomera, Australia.

Some data, uncorrected for Earth albedo variation, from this long-term period are:

Tilt angle, deg	Percent of data time
0 to 6	47.0
3 to 8	37.6
6 to 16	14.5
14 to 19 [a]	0.9

[a] See discussion of anomalous data for orbit 87.

Uncorrected data collected during orbit 109, a north-to-south pass from Hybla Valley, Va., to Quito, Ecuador, which furnished the longest continuous "look" at the satellite, are:

Tilt angle, deg	Duration, sec
0 to 6	588
3 to 8	472
0 to 6	128
	Total: 1188

One anomalous series of data points was observed. On orbit 87, Woomera, Australia, recorded the following data:

Tilt angle, deg	Duration, sec
3 to 8	118
6 to 16	304
14 to 19	196
6 to 16	227

Note that a telemetry indication of tilt angle between 6° and 16° is followed by a 3-minute indication of 14° to 19° and finally an indication of 6° to 16°. If the one assumption is made that the sensor farthest away from the local vertical is triggering because of internal reflections from a bright spot on Earth (i.e., cloud), this telemetry indication can be corrected to mean a tilt angle between 6° and 16°. It is thought that no such cloud-cover information is available. The universal time for this observation was 18 days, 02 hours, 29 minutes, and 40 seconds, 1964. The subsatellite point is 31° South latitude and 152° East longitude. Any cloud-cover information that can be made available for this data point will be appreciated.

Because of the low sensor resolution and albedo sensitivity, a careful review is required to determine the peak misalinement angle. On the basis of the percent of time in the various error angle bands, the system appears to follow the behavior predicted by analytical studies made prior to flight. It may safely be deduced from the uncorrected data that the peak steady-state pointing error is less than 10° and the system is performing within specifications.

A point-by-point study of the data revealed large values of earth albedo in the sensor viewing area for all cases where tilt angles were indicated to be larger than 6° and earthlighting conditions could be checked by albedo contour measuring systems aboard other satellites. Tiros photographic data also indicated bright earthlight conditions during these periods. A calibration on flight backup aspect sensors proved that erroneous triggering does occur for large albedo values. On the basis of data corrected for false sensor triggering, a peak pointing error of 6° is the maximum observed. The data reduction effort has been continued through the date of this report. No data have been collected to change the original conclusion on pointing accuracy.

Experiment II

The time of launch for experiment II was selected so that the satellite would be injected into an orbit which was most favorable for observing optical aspect data. Data remained optimum for 2 weeks after launch. Hybla Valley, Va.; Lompoc, Calif.; Lima, Peru; Santiago, Chile; Woomera, Australia; and Winkfield, England, tracked experiment II

during phases of optimum earthlight conditions.

An overwhelming amount of data were lost because of limited ground-station coverage, and some of the recovered data are useless for data reduction because of poor earthlighting conditions. As an example, the data which we have for the first 192 orbits after boom extension correspond to slightly less than 340 minutes of flight time. However, we have only 156 minutes of useful data, that is, data with bright earthlighting conditions. This is only 0.79 percent of flight time.

The satellite attitude at the time of boom extension is unknown. After 13 orbits, pitch and roll motions had decayed to less than 10°. The longest nearly continuous aspect data collected during one pass are shown in figure 19. These data were collected during a southbound pass from Hybla Valley, Va., to Lima, Peru.

Six days after boom deployment the satellite was inverted from the boom-down to the boom-up position. The maneuver was performed by simply retracting the boom from the fully extended length of 41 feet to an intermediate length of 20 feet. Because of conservation of angular momentum, the satellite pitch rate increased from 1 revolution per orbit to slightly over 4 revolutions per orbit. The boom retraction was followed by a coast phase which allowed the boom to rotate from the vertically downward position to the nearly vertically upward position. The boom was then reextended to its full length of 41 feet to decrease the pitch rate to 1 revolution per orbit at the same time the boom pointed vertically up. The time sequence for the maneuver is shown in figure 20. Because of command-station locations the maneuver was performed at night. The next daylight orbit indicated no change in stabilization-system performance accuracy. Steady-state oscillations were less than 7°; this indicated that disturbances had been small and/or had decayed in 5 orbits. Two days after the first inversion another maneuver was performed. This maneuver returned the satellite back to

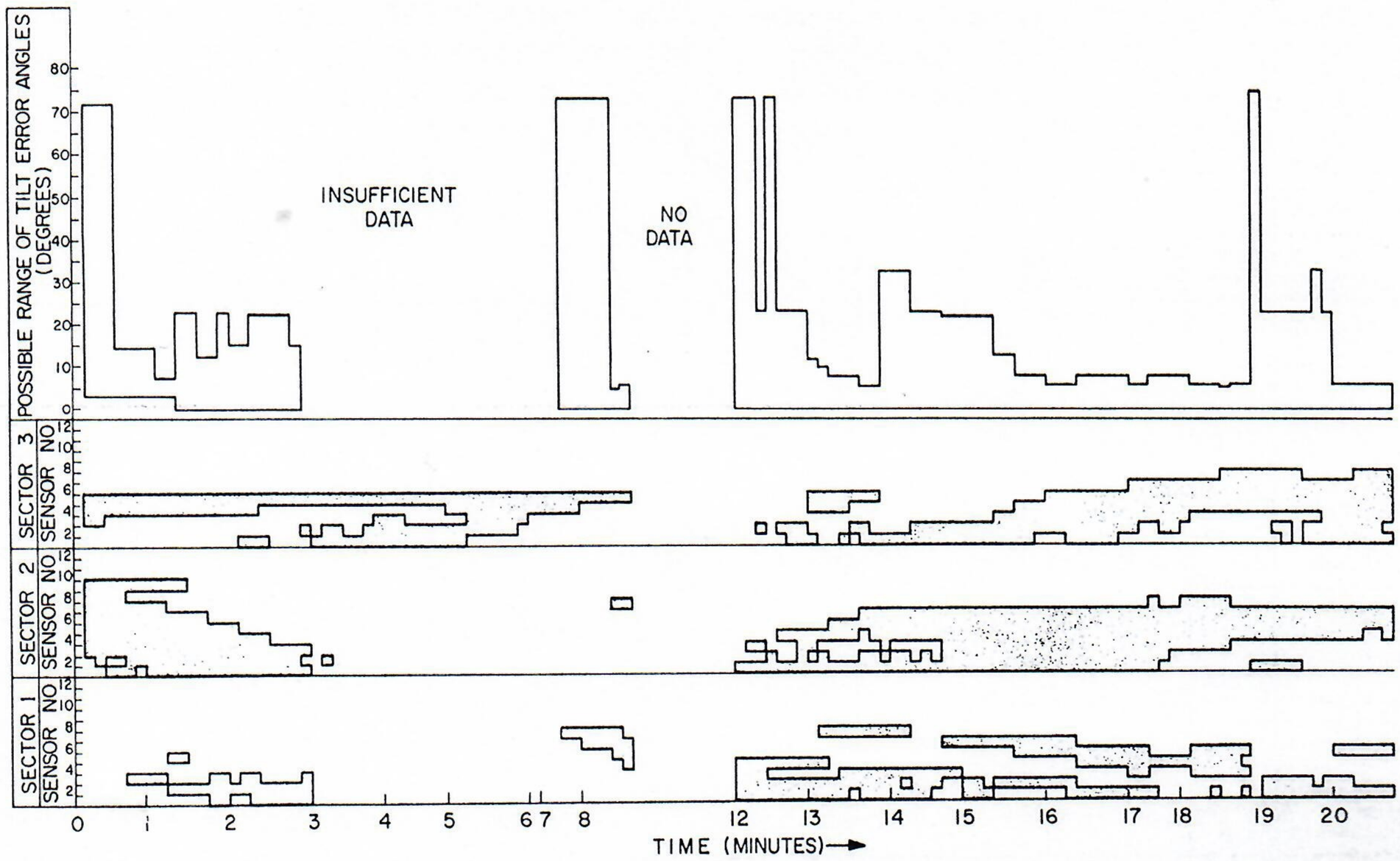

FIGURE 19.—Longest continuous aspect data collected by experiment II.

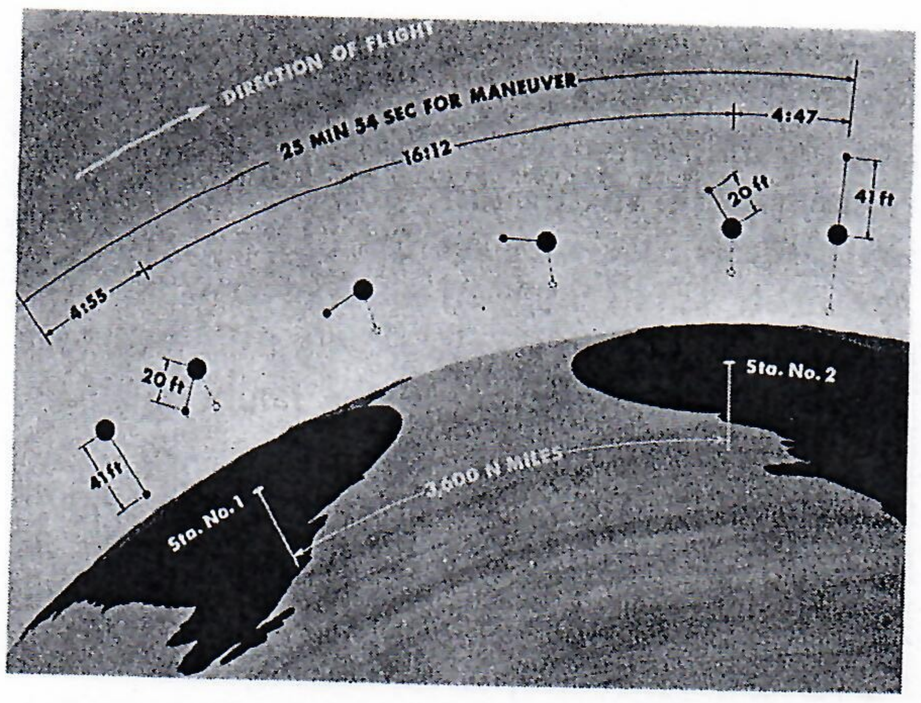

FIGURE 20.—Inversion maneuver sequence for experiment II.

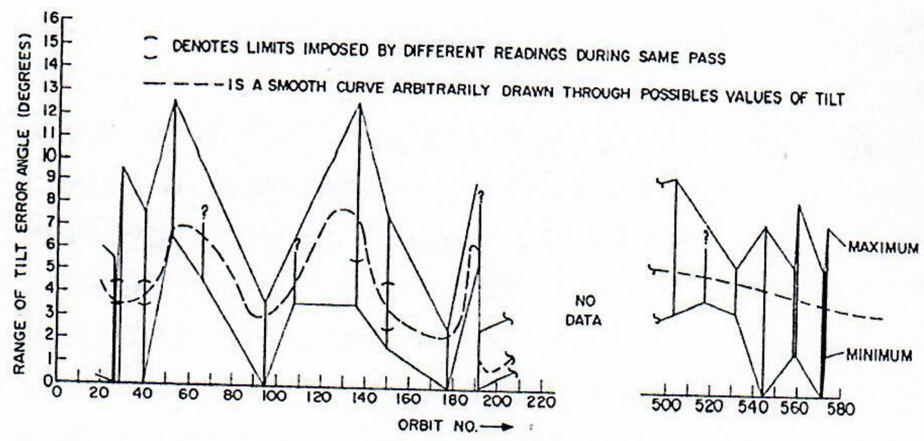

FIGURE 21.—Time history of system performance.

the boom-down position with the same procedure and resulting accuracies. The inversion may be tried again on this satellite at some future date to check hardware performance after a prolonged exposure to the space environment. The high degree of repeatability in boom operation on the ground and in flight and the small oscillation angles experienced because of the inversion maneuvers have proven the practicality of this extremely simple and useful inversion system. Pointing accuracies of no worse than 7° and as good as 3° are indicated after the inversion. The

RANGE OF TILT ERROR ANGLE	% OF EACH CATEGORY	TILT ERROR ANGLE 2-1/4	3-1/2	4-1/2	5-1/2	6-1/4	7-1/2	9-1/2	11-1/2	12-1/2	14-1/2
0 - 2-1/4	5.67	5.67									
0 - 3-1/2	10.5		16.17								
0 - 4-1/2	19.97			40.48							
1-3/4 - 4-1/2	3.97										
2-1/2 - 4-1/2	0.37										
0 - 5-1/2	23.83				67.91						
1-3/4 - 5-1/2	2.84										
3-1/2 - 5-1/2	0.76										
0 - 6-1/4	1.13					69.41					
2-1/2 - 6-1/4	0.37										
0 - 7-1/2	11.63						82.33				
1-3/4 - 7-1/2	0.76										
3-1/2 - 7-1/2	1.13										
0 - 9-1/2	5.67							91.44			
1-3/4 - 9-1/2	2.84										
0 - 11-1/2	2.13								93.57		
0 - 12-1/2	1.798										
3-1/2 - 12-1/2	2.84									98.59	
6-1/2 - 12-1/2	0.38										
3-1/2 - 14-1/2	1.418										100.0

FIGURE 22.—Refined time-history data.

21-foot reduction in boom length for the inversion maneuver was chosen to maintain pointing accuracies to within 10° of the vertical had the boom failed to reextend.

Figure 21 is a time history of system performance. Pass number is plotted against possible range of tilt angle (as indicated by the vertical lines). Again, the range of tilt angle does not mean that the angle varies over the entire range, but only that the angle lies somewhere within the range. The dotted line is merely a smooth curve drawn through the possible values of angles and is consistent with theoretical predictions.

Figure 22 further summarizes figure 21. The criterion used in selecting these data was that they had both upper and lower limits for the tilt angle. Maximum tilt angles are represented horizontally. The second ordinate column represents the percent of total data contained in each separate category of angle ranges which are tabulated in the first column. The bar graph shows the cumulative range of error angle. Maximum tilt angles are represented across the top of the figure. Tilt-angle ranges are represented in the ordinate. Although 14½° peak error angles are possible interpretations from this figure, they may be discarded since they are typically bracketed by error bands with maximum tilt error angles of less than 5½°. When the earthlight conditions are of maximum brightness in the sensor viewing area, maximum resolution occurs. During these periods of high resolution peak pointing errors of less than 6° are always observed. It is only when data resolution is poor that the upper limit of the error band is about 6°.

The successful stabilization of both experiments I and II has proven the practicality of pointing accuracies to within 10° based upon raw data and 6° based upon corrected data.

Experiment III

Performance data on experiment III are not available because of a change in the computer data reduction program. Prior to launch, the combination of the Earth optical and magnetic systems was considered the best choice of high resolution data. Identical low-sensitivity problems in the optical system of this satellite, as in experiment II, became apparent after launch. Therefore, it was necessary to ask NWL to reprogram their computer to accept solar and magnetic data. This program has been written and is in the debugging stage.

☆ U. S. GOVERNMENT PRINTING OFFICE: 1966—O 212-746